Impact of intermittent electricity supply on a conceptual process design for microbial conversion of CO_2 into hexanoic acid

Luo, Jisiwei; Pérez-Fortes, Mar; Ibarra-Gonzalez, Paola; Straathof, Adrie J.J.; Ramirez, Andrea

DOI
10.1016/j.cherd.2024.04.005

Publication date
2024

Document Version
Final published version

Published in
Chemical Engineering Research and Design

Citation (APA)
Luo, J., Pérez-Fortes, M., Ibarra-Gonzalez, P., Straathof, A. J. J., & Ramirez, A. (2024). Impact of intermittent electricity supply on a conceptual process design for microbial conversion of CO_2 into hexanoic acid. *Chemical Engineering Research and Design*, *205*, 364-375. https://doi.org/10.1016/j.cherd.2024.04.005

Chemical Engineering Research and Design 205 (2024) 364–375

Contents lists available at ScienceDirect

Chemical Engineering Research and Design

journal homepage: www.elsevier.com/locate/cherd

Impact of intermittent electricity supply on a conceptual process design for microbial conversion of CO_2 into hexanoic acid

Jisiwei Luo [a,*], Mar Pérez-Fortes [a], Paola Ibarra-Gonzalez [a], Adrie J.J. Straathof [b], Andrea Ramirez [c]

[a] Department of Engineering Systems and Services, Faculty of Technology, Policy and Management, Delft University of Technology, Jaffalaan 5, Delft 2628BX, the Netherlands
[b] Department of Biotechnology, Faculty of Applied Sciences, Delft University of Technology, van der Maasweg 9, Hz Delft 2629, the Netherlands
[c] Department of Chemical Engineering, Faculty of Applied Sciences, Delft University of Technology, van der Maasweg 9, Hz Delft 2629, the Netherlands

ARTICLE INFO

Keywords:
Process design
Microbial electrosynthesis
Hexanoic acid
Intermittent renewable electricity
Volume flexibility
Techno-economic assessment

ABSTRACT

Combining intermittent renewable electricity (IRE) with carbon capture and utilisation is urgently needed in the chemical sector. In this context, microbial electrosynthesis (MES) has gained attention. It can electrochemically produce hexanoic acid, a value-added chemical, from CO_2. However, there is a lack of understanding regarding how the intermittency of renewable electricity could impact the design of a MES plant. We studied this using Aspen Plus models.

A MES plant that was powered by constant grid electricity could operate from 100% down to 70% of its nominal capacity, at which point the heat exchangers and the internal geometrical design of the distillation towers became bottlenecks. The levelised production cost of hexanoic acid (LPC_{C6A}) was estimated at 4.0 €/kg. Switching to IRE supply increased LPC_{C6A} to 5.3 €/kg (for wind electricity) and 4.7 €/kg (for hybrid renewable electricity).

A battery energy storage system (BESS) was deployed. The lowest LPC_{C6A} was found at a BESS installation of 29 GJ/h for wind electricity (5.1 €/kg) and at 12 GJ/h for hybrid renewable electricity (4.7 €/kg). In both situations, the volume flexibility of the MES plant was not improved. At the investigated market and operating conditions, coupling IRE to the MES plant was economically infeasible.

1. Introduction

According to the IPCC Sixth Assessment Report, it is still possible to reach the 1.5 °C climate goals (IPCC, 2022). This, however, requires immediate and profound changes across different sectors. As a major emitter of greenhouse gases, the chemical sector should take urgent measures to reduce its emissions. A potential option is to accelerate the transition from fossil to renewable energy and shift to technologies that use low-carbon feedstocks and energy streams (Morgenthaler et al., 2020).

By having the potential to combine intermittent renewable electricity (IRE) with carbon capture and utilisation (CCU), electrochemical CO_2 utilisation has drawn significant attention in the chemical sector. Lately, microbial electrosynthesis (MES) has come into sight for its ability to convert CO_2 into volatile carboxylic acids (VCAs), such as formic, acetic, butyric acids, and hexanoic acid (Del Pilar Anzola Rojas et al., 2018; Prevoteau et al., 2020). Formic acid requires two electrons (2 e^-) when the faradaic efficiency (FE) is 100 % and an electric energy of 3.88 kWh/kg at a FE of 90 %. Similarly, acetic acid needs 8 e^- and 11.89 kWh/kg. Butyric acid asks for 20 e^- and 20.28 kWh/kg. Hexanoic demands 32 e^- and 24.60 kWh/kg (Prevoteau et al., 2020). Among all, hexanoic acid, also known as *n*-caproic acid, has the highest market price (i.e., 2.5–4.2 €/kg (Dessi et al., 2021)) (Jourdin et al., 2020). Unlike the others, hexanoic acid only has one industrial production method, which is the fractional distillation of coconut or palm kernel oil. Additionally, it is a by-product accounting for less than 1 wt% (Canapi et al., 2005). Hence, its availability is constrained by the production of these two plant oils. Subsequently, it is subjected to disruptions in both markets caused by, for example, weather (Whitehead, 2017) or export bans (The Dollar Business Bureau, 2017). However, high-purity hexanoic acid (i.e., >98 wt%) has a wide range of important applications, such as animal feed additive, flavour additive, and chemical raw material (Cavalcante et al., 2017). The use of MES has the potential to

* Corresponding author.
E-mail address: J.Luo-1@tudelft.nl (J. Luo).

https://doi.org/10.1016/j.cherd.2024.04.005
Received 22 November 2023; Received in revised form 1 February 2024; Accepted 4 April 2024
Available online 10 April 2024

Nomenclature

Symbols

Jin_t	Electricity stored in the BESS at time *t*, GJ/h
$Jout_t$	Electricity discharged from the BESS at time *t*, GJ/h
J_t	Electricity consumption immediately used for hexanoic acid production at time *t*, GJ/h
P_t	Available electricity from the wind and/or solar farm at time *t*, GJ/h
V	Vector of hourly available electricity over hourly nominal electricity consumption (for intermediate calculation), %
A	Heat exchange surface area, m^2
C_v	Yearly coverage percentage of shortage hours at an available electricity power *v*,%
E	Electricity cost, M€/y
F	Feedstock cost, M€/y
J	Electricity consumption, GJ/h
$\dot{M}$	Mass flow rate at plant level, kt/y
$\dot{m}$	Mass flow rate at equipment level, t/h
n	Plant lifetime, years
Q	Heat duty, kJ/s
r	Discount rate, %
$Temp$	Temperature of the hot stream, K
$temp$	Temperature of the cold stream, K
U	Overall transfer coefficient, kJ/(s m^2 K)
UT	Utility cost at plant level, M€/y
v	Available electricity power generated by the wind and/or solar farm (time-independent), GJ/h
v^*	Available electricity power generated by the wind and/or solar farm (time-independent; for intermediate calculation), GJ/h
WT	Waste treatment cost, M€/y
$\mathbb{Z}$	Integers
θ	Price, €/kg
Φ	Statement inside the Iverson bracket

Superscripts

H	Hybrid renewable electricity
i	Type of equipment (for volume flexibility analysis)
k	Case number, from 0 to 6
W	Wind electricity

Subscripts

C6A	Hexanoic acid
in	Inlet
LB	Lower boundary
max	Maximum value
min	Minimum value
o	Nominal condition of the reference process
O2	Oxygen
out	Outlet
t	Time, h
T	Time, h (1–8760 h)
UB	Upper boundary
y	Year

Acronyms

AF	Allocation factor
BESS	Battery energy storage system
CAPEX	Capital expenditure, M€/y
CCU	Carbon capture and utilisation
DSP	Downstream processing
FE	Faradaic efficiency
IRE	Intermittent renewable electricity
LLE	Liquid-liquid extraction
LMTD	Log-mean temperature difference, K
LPC	Levelised production cost, €/kg
LRR	Load ratio range, %
MES	Microbial electrosynthesis
O&M	Operation and maintenance cost, M€/y
OPEX	Operating expenditure, M€/y
REC	Range of effective capacity, %
SCCAs	Short-chain carboxylic acids
SR	Solvent regeneration
TD	Dehydration column
TOA	Trioctylamine
TRL	Technology readiness level
VCAs	Volatile carboxylic acids
TD	Dehydration column

decouple the production of hexanoic acid from biomass and vegetable oils and expand what until now has been a niche market due to limited natural resources. For instance, as a longer carboxylic acid, hexanoic acid can be upgraded to a blend in sustainable aviation fuels via ketonisation and hydrodeoxygenation (Huq et al., 2021; Miller et al., 2022).

As with any other electrochemical technology, MES can run flexibly on a fluctuating electricity supply (Chen et al., 2019; De Luna et al., 2019; Zhang and Tremblay, 2019). However, the MES unit is simply part of a process. To meet product requirements, downstream processing (DSP) also plays a vital role. Since MES produces hexanoic acid in a dilute environment, rigorous DSP is required to reach a high-purity product stream. Published recovery and purification technologies for separating VCAs, such as hexanoic acid, from water, are energy-intensive and or costly (Aghapour Aktij et al., 2020; Atasoy et al., 2018; Jones et al., 2021). They include distillation, reactive distillation, adsorption, electrodialysis, solvent extraction, nanofiltration, reverse osmosis, and membrane separation; and combinations thereof. Novel methods like capacitive deionization are also being explored in this area (Valentino and Alejandre, 2023). Woo and Kim (2019) modelled the recovery and purification of VCAs, including hexanoic acid, from a dilute aqueous stream in Aspen HYSYS. Their selected recovery method was liquid-liquid extraction (LLE), using nonyl acetate and hexyl acetate as solvents, followed by distillation. Saboe et al. (2018) experimentally performed extraction of hexanoic acid from a dilute stream using solvents Cyanex 923 and trioctylamine (TOA) in membrane-based LLE and following solvent regeneration. They also simulated solvent regeneration and ambient distillation units in Aspen Plus. Benalcázar et al. (2017) simulated LLE of hexanoic acid with n-decane and subsequent purification by distillation in Aspen Plus. The overall recovery yield of hexanoic acid in these three studies was above 90 %, and its purity was above 99 wt%.

However, the abovementioned DSP technologies have been developed for steady and continuous operations. Integrating IRE to an electrochemical plant will introduce fluctuations to the throughput rates of the DSP. A common tool to handle fluctuations is “flexibility” (Ajah and Herder, 2005; Grossmann and Sargent, 1978; Luo et al., 2022). For coping with fluctuations in electricity supply and consequently volume/mass flowrates, the flexibility type desired is volume flexibility (Luo et al., 2022). It is defined as the ability, at a hierarchical level (i.e., equipment, process route, or plant), to operate over a range of throughput rates on a given timescale basis (e.g., per second, per month) to cope with a target (e.g., variations in feedstock quantity) without unacceptable impacts (e.g., profitability). Incorporation of volume flexibility in the process design should lead to the operating window that

guarantees the proper function of an electrochemical plant powered by IRE.

Nonetheless, literature provides limited insights into the implications of incorporating intermittency and subsequent volume flexibility in the design of chemical processes, especially for technologies that are currently at a low technology readiness level (TRL), such as the MES technologies that are at a TRL of 2–3. Depending on the types of microorganisms, MES technologies can take in different feedstock and synthesise various products. The technical and/or economic performances of some MES technologies at the plant level have been evaluated by ex-ante assessments, though under constant power supply (Christodoulou and Velasquez-Orta, 2016; Gadkari et al., 2021; Jourdin et al., 2020; Sadhukhan et al., 2016; Shemfe et al., 2018; Wood et al., 2021). For instance, Christodoulou et al. (2017) estimated the production cost of direct conversion of CO_2 into formic, acetic, and propionic acids, methanol, and ethanol, respectively. Only formic acid and ethanol were reported to have a lower production cost than their market value when simply the assumed cheaper price but not the real intermittency of renewable electricity was considered. Shemfe et al. (2018) assessed the production cost the formic acid converted from CO_2, between 5–15 €/kg, which is lower than the market price. Nonetheless, the DSP was not included in their process system. Wood et al. (2021) evaluated a range of products synthesised straight from CO_2 directly captured from air. The production costs are significantly higher than their market value. Jourdin et al. (2020) examined the hexanoic acid production directly from CO_2 and short-chain carboxylic acids (SCCAs), respectively. Both the capital and operating costs of generating hexanoic acid from CO_2 are much lower than from SCCAs. However, the net present value is negative even without considering the cost of DSP. Promoting the electron selectivity towards hexanoic acid to 100% would turn the process that encompasses the DSP profitable.

Up to date, the impact of IRE on the MES operation has only been investigated at a lab scale (Del Pilar Anzola Rojas et al., 2018) whereas the impact of IRE in the design of a MES plant is unknown. Beyond MES, some Power-to-Chemicals studies have considered design strategies for enhancing volume flexibility at different stages of TRL, for example (Brée et al., 2020; Chen and Yang, 2021; Huesman, 2020; Osman et al., 2020; Qi et al., 2022; Wang et al., 2020). For instance, Brée et al. (2020) considered five strategies to enhance the volume flexibility of a conventional chlor-alkali process against the variable electricity supply: (i) oversizing the equipment; (ii) adopting a more flexible conversion technology; (iii) installing storage tanks; (iv) incorporating a water electrolyser or fuel cell; (v) implementing a battery energy storage system (BESS). They concluded that, in their case, a more flexible technology economically performed better than a less flexible technology assisted by a BESS. In another example, Huesman (2020) adopted a BESS to improve the flexibility of a methanol plant using CO_2 from direct air capture and H_2 from water electrolysis coupled with solar power, but the resulting penalty in the manufacturing cost was high. The intuitive approach to improve flexibility with a BESS seemed again hardly helpful, particularly regarding the economics. Nonetheless, it is uncertain if this ineffectiveness of installing a BESS also applies to other electrochemical production systems.

Given the importance of an alternative production route of hexanoic acid and flexible operation of electrochemical processes coupled with IRE, this paper aims to contribute to the methodological approach for designing and assessing flexible processes at a low TRL, using microbial electrosynthesis of hexanoic acid as the only conversion technology. This work conducts an ex-ante assessment to evaluate the potential techno-economic performances of this specific MES technology, assuming it is available today. A plant centred on this specific MES technology and powered by IRE supply is designed. The DSP of the MES plant will rely on membrane-based LLE with TOA, vacuum distillation, and ambient distillation. In addition, as a strategy for enhancing volume flexibility of the MES plant, a BESS will be deployed in the plant.

2. Methodology

2.1. Process system

2.1.1. Design consideration

The nominal production capacity of hexanoic acid was fixed at ca. 10 kt/y. The MES plant was designed to obtain an overall recovery yield of 99.8 % of hexanoic acid at 99 wt% purity in liquid form. The remaining 1 wt% of the composition consists of water, acetic acid, butyric acid, and the extraction solvent. Due to the reaction stoichiometry, pure oxygen was produced as a by-product, at ca. 22 kt/y (Jourdin et al., 2020).

The plant was assumed to be located in the Port of Rotterdam, the Netherlands. With construction starting in 2018 and operation in 2019, the lifetime of the plant was assumed to be 30 years (Jourdin et al., 2020). Equipment with a shorter lifetime was assumed to be replaced after 15 years of operation.

Furthermore, it was assumed that feedstock except for electricity was supplied as needed and that the product was delivered to the market without further packing or conditioning.

2.1.2. Process description

The MES unit was designed on basis of experimental data used in (Jourdin et al., 2020). The DSP was designed based on experimental and exhaustive Aspen Plus simulation results of a similar system in (Saboe et al., 2018). Fig. 1 is a simplified block flow diagram of the plant. Purge streams, heat exchangers, and centrifuges have been omitted from the figure for simplicity.

MES is driven by electricity. A BESS is installed prior to it, to buffer fluctuations in the electricity supply. Demineralised H_2O feeds the anode compartment of the MES, while demineralised H_2O, pure CO_2, and $Ca(OH)_2$ enter its cathode compartment. In the anode chamber, H_2O is split into O_2 and H^+. O_2 is vented from the headspace of the anode chamber. All H^+ passes though the membrane to the cathode compartment. The outlet stream of the cathode compartment contains aqueous acetate, butyrate, hexanoate, and their corresponding acids. The purity of the carboxylates and carboxylic acids is in total 1 wt% (Jourdin et al., 2020). This outlet stream is acidified using aqueous H_3PO_4 to precipitate Ca^{2+} as $CaHPO_4$, which is removed using a centrifuge. The liquid stream from the acidification unit is sent to a membrane-based LLE (LLE1) that uses trioctylamine (TOA) as extracting solvent (Saboe et al., 2018). The extract stream is pre-heated before entering a vacuum solvent regeneration column (SR1). TOA from the bottom of SR1 is recycled to the LLE1. The overhead stream of SR1 contains carboxylic acids and water in a higher mass purity than in the outlet stream of the acidification unit. However, after a single extraction unit, this ratio is still below the azeotropic composition. Therefore, the overhead stream from SR1 is fed to a second membrane-based LLE with TOA as solvent (LLE2). The extract stream from LLE2 is pre-heated, centrifuged to remove salt precipitate, and sent to a second solvent regeneration column (SR2). The bottom stream from SR2 contains TOA and is recycled to LLE2. The overhead stream of SR2 is sent to a dehydration column (TD). Short-chain carboxylic acids (i.e., acetic and butyric acids) and water are separated from the hexanoic acid as distillate, and this distillate is recycled to the MES. The bottom stream of the dehydration column is the hexanoic acid stream, which is centrifuged to remove remaining salt precipitate and cooled to room temperature. The final product stream is liquid hexanoic acid at 99 wt% purity. The two raffinate streams (from LLE1 and LLE2) and the distillate stream from the dehydration unit are cooled and recycled to the cathode compartment of MES, to enhance the overall yield of hexanoic acid on CO_2. A more detailed process description is presented in Appendix A, and the process flowsheet can be found in Appendix B.

2.1.3. Modelling approach and key assumptions

A non-random two-liquid thermodynamic model was chosen as the

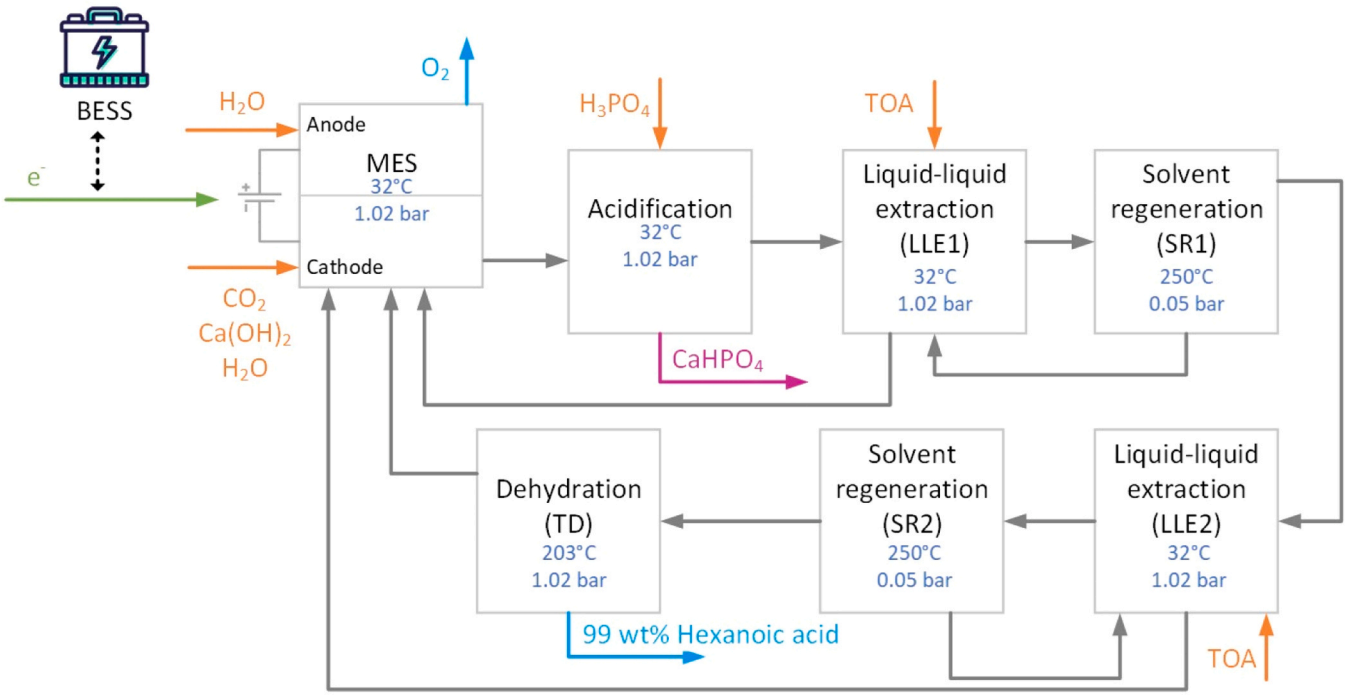

Fig. 1. Simplified block flow diagram of the MES plant. MES: microbial electrosynthesis; LLE: liquid-liquid extraction; SR: solvent regeneration; TD: dehydration column; TOA: trioctylamine.

global property method with the Hayden-O'Connell equation of state for vapour phase properties, namely NRTL-HOC, in Aspen Plus v12 (referred to as Aspen hereafter). This thermodynamic property package can deal with dilute electrolyte streams and carboxylic acids.

MES has not been made a built-in model in Aspen. A dynamic computation model of MES could be incorporated into the simulation to enhance the accuracy (Gadkari et al., 2019). However, the kinetic data of the MES producing hexanoic acid is not available yet. Hence, it was modelled as a black box using an RYield model in Aspen, controlled by Fortran codes in a calculator block. It represents the MES by its mass balance, energy balance, and process parameters. All information, such as operating conditions, electron selectivity, productivity, and purity of the MES is based on (Jourdin et al., 2020) and their previous experimental work cited therein. Details are compiled in Appendix B. The three heat-based distillation columns (i.e., SR1, SR2, and TD) were modelled using built-in RadFrac models with condenser and reboiler. The vacuum needed for the two vacuum solvent regeneration units (i.e., SR1 and SR2) was generated by ejectors which were driven by medium-pressure steam; these were modelled by expanders in Aspen, in the absence of ejectors. Their energy consumption and sizes were estimated based on the operating conditions from (Saboe et al., 2018) and are summarised in Appendix A. The two LLE units should be two membrane contactors (Saboe et al., 2018). They were modelled as two extraction towers. Salt was assumed to be completely removed by a filter before the main stream entered LLE1. The local property method selected for both LLE units was the universal quasichemical functional-group activity coefficients with the Hayden-O'Connell equation of state for vapour phase properties (UNIFAC-HOC). Further modelling assumptions and details about the process are provided in Appendix A.

Heat was consumed or generated as utilities, such as low-pressure steam and hot oil. The same type of utilities consumed and generated were subtracted. Note that heating was always a one-time process while cooling was staged. Furthermore, electricity was integrated.

The BESS and IRE profiles were not directly modelled in Aspen. Section 2.5 explains their integration with the process model.

Given the TRL of MES and membrane-based LLE, it is challenging to validate the simulation results of the whole process configuration without experiments or pilots. However, we carried out a sanity check at the unit level with the help of analogous literature, technology developers, and industrial experts. See more details in Appendix A.

2.2. Electricity supply profiles

Three electricity supply profiles were considered. One supplied constant grid electricity at the nominal electricity consumption rate of the MES plant ("J_o"; GJ/h). The other two were IRE profiles: 1) wind electricity from an onshore wind park, and 2) hybrid renewable electricity supply consisting of the same wind park together with an additional solar farm. The IRE profiles were generated on basis of Rotterdam's wind speed and solar radiation data with an hourly interval over 2019 (8760 hours). The raw data was initially retrieved as hourly capacity factors from (Staffell and Pfenninger, 2016). They were then converted into energy per hour by multiplying with the peak capacities of the selected wind park (Windpark Slufterdam, the Netherlands; 50.4 MWp) (Eneco, 2022), and the solar farm (Shell Moerdijk, the Netherlands; 27 MWp) (Shell, 2019). A direct line was assumed between the MES plant and the solar and wind farms. Furthermore, the solar and wind farms were built primarily to support the MES plant. With these assumptions, the renewable origin is guaranteed and the additionality condition is met following the latest regulations of the European Union (Commission Delegated, 2023). Also, it was assumed that the renewable electricity farm did not supply electricity to the MES plant as per demand. Instead, the intention was to explore how much available electricity from the renewable electricity farm the MES plant could consume. The electricity the plant could not consume was simply not used by the plant. The IRE profiles were represented by two datasets of 8760 data points each, "P_t^W" (GJ/h) for the wind power supply data and "P_t^H" (GJ/h) for the hybrid power supply data. The values were treated such that "P_t^W/J_o" " and "P_t^H/J_o" have a precision of 1%. Details can be found in Appendix B.

The price of the constant grid electricity was assumed as the average electricity wholesale price for industrial use in the Netherlands in 2019,

i.e., 25.56 €/GJ (Statista, 2019). For the hypothetical future pricing scheme of the renewable electricity, two three-tier load-following pricing schemes were assumed for the two IRE profiles, mimicking a power purchase agreement. The pricing scheme of the wind electricity profile is illustrated in Fig. 2. It was determined based on both load and time. Peak hours were assumed to be 30 % of the time in a year when the capacity factor was the lowest. Off-peak hours were assumed to be 30 % of the time in a year when the capacity factor was the highest. Mid-peak hours were assumed to be 40 % of the time in a year when the capacity factor was in the middle. The off-peak, mid-peak, and peak prices were assumed to be 85 %, 100 % and 115 % of that of the constant grid electricity, respectively (McNamara et al., 2022). The same rationale was applied to the hybrid renewable electricity profile. Furthermore, it was assumed that the electricity profiles and their pricing schemes were the same throughout the 30 years of the plant's lifetime. Details pertaining to the pricing are presented in Appendix B.

2.3. Operating schemes

Operating scheme 1 followed four rules, specified for the hourly operation of the plant together with the BESS:

1) when the total electricity available from the IRE and the BESS does not reach the minimum tolerable throughput rate of the plant (how it was obtained is explained in Section 2.5.1), shut down the production;
2) otherwise, ensure the minimum tolerable throughput rate of the plant, if needed, with the backup electricity from the BESS;
3) if the BESS is not fully charged and not used for production, charge it;
4) if the BESS is fully charged, increase the production of the plant using IRE directly.

Operating scheme 2 proposed that:

1) when the total electricity available from the IRE and the BESS does not reach the minimum tolerable throughput rate of the plant, shut down the production;
2) otherwise, boost the production as much as possible, by using the backup electricity from BESS in addition to IRE;
3) if the BESS was not fully charged, only charge it during off-peak hours when the two prior rules were satisfied.

A critical assumption was that the ramping time was negligible. Details about the two operating schemes are schematically illustrated in Appendix A.

2.4. Cases

In total, seven cases were examined, as summarised in Table 1. In each case, the BESS implementation, electricity supply profile, and the operating scheme of the plant were specified if applicable.

2.5. Volume flexibility estimation

To integrate the Aspen process model with the BESS, the electricity profiles, and the two operating schemes, Python scripts were created. They were used to extract mass and energy balances of the process model from Aspen at varying throughput rates and to assess techno-economic performances.

To design for or assess any type of flexibility, five elements have to be specified for the context, namely hierarchical level, target, range, time scale, and impacts (Luo et al., 2022). As has been stated in Section 1, this work focuses on the volume flexibility of the MES plant. However, to evaluate the volume flexibility at the plant level in Cases 1–6, we first need to understand the volume flexibility at the equipment level independent of any case. Hence, the five elements are specified for the volume flexibility at both the equipment and plant levels (see Table 2).

At equipment level, volume flexibility is defined as the ability of the equipment to operate within a range of flow rates while meeting the product and design requirements. It was characterised by the range of effective capacities (REC), which is elaborated on in Section 2.5.1.

At the plant level, volume flexibility is represented by the range of electricity available from the renewable electricity farm that the plant could fully consume while meeting product requirements without damaging the equipment. It was characterised by the load ratio range

Table 1
Summary of cases the plant level considered in this work. BESS: battery energy storage system.

Case	Electricity supply profile	BESS implementation	Operating scheme
0	Grid	No	-
1	Wind	No	-
2	Hybrid	No	-
3	Wind	Yes	1
4	Hybrid	Yes	1
5	Wind	Yes	2
6	Hybrid	Yes	2

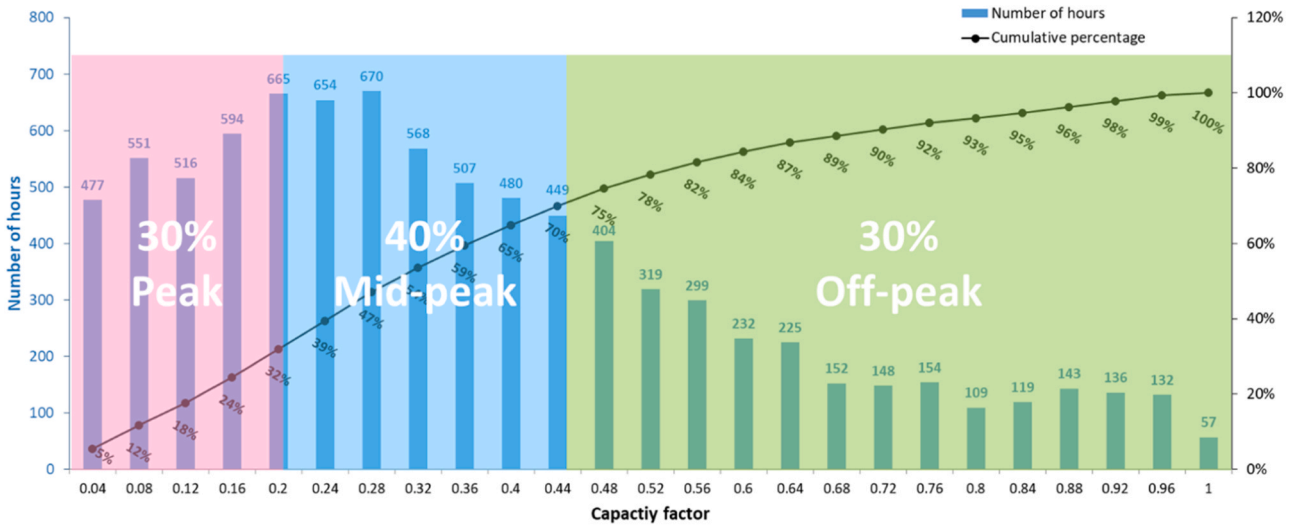

Fig. 2. Three-tier load-following pricing scheme used for wind electricity.

Table 2
Definitions of volume flexibility used in this work, based on (Luo et al., 2022). REC: range of effective capacities. LRR: load ratio range.

Element	Specification	
Hierarchy level	Equipment	Plant
Target (unit)	Fluctuating throughput rates (kg/h)	Fluctuating electricity supply (GJ/h)
Range (unit)	REC (%)	LRR (%)
Time scale	Hourly	Hourly
Impacts/ conditions	• Meeting the product requirements • Not damaging the equipment	• Fully consuming electricity available from wind and/or solar farm • Meeting the product requirements • Not damaging the equipment

(LRR). LRR is impacted by REC. Moreover, LRR is also associated with other factors such as electricity supply profiles and operating schemes of the plant. LRR is further detailed in Section 2.5.2.

Additionally, the precision of both REC and LRR was set as 1 % in this work.

2.5.1. Equipment level

REC^i, as calculated by Eq. (1), represents the minimum "$\dot{m}^i_{\min}$" and maximum "$\dot{m}^i_{\max}$" tolerable throughput rates a piece of equipment "i" could handle. Values are normalised to the nominal value "$\dot{m}^i_o$" (Luo et al., 2022). The larger the range, the higher the flexibility of the equipment, i.e., the larger the range of throughput rates at which each equipment operates safely while satisfying the designed recovery yield and purity of hexanoic acid. The limits were detected by failures to meet product requirements, temperature requirements for heat exchangers, or experiencing unstable hydraulics of tower trays. In this work, the assessment of volume flexibility at the equipment level focused on three heat-based distillation columns (i.e., SR1, SR2 and TD), because their operating conditions such as temperature and pressure are more complex and stringent. The rest of the equipment was assumed to be fully flexible without loss in performance or penalty in energy consumption.

$$REC^i = [\frac{\dot{m}^i_{\min}}{\dot{m}^i_o}, \frac{\dot{m}^i_{\max}}{\dot{m}^i_o}] \tag{1}$$

where,

REC^i, range of effective capacity, %
i, equipment, i.e., SR1, SR2, or TD here
$\dot{m}^i_{\min}$, minimum tolerable throughput rate for equipment i, kg/h
$\dot{m}^i_o$, nominal tolerable throughput rate of equipment i, kg/h
$\dot{m}^i_{\max}$, maximum tolerable throughput rate for equipment i, kg/h

To determine REC^i, the throughput rates should be varied while the dimensions of the columns were fixed at the nominal conditions in the Aspen model. Nonetheless, in Aspen, equipment is by default automatically resized when the throughput rate varies. In a built-in RadFrac model with integrated condenser and reboiler, the dimension of a column can be manually fixed by specifying the tray diameter, tray spacing, etc. However, the dimensions of the integrated condenser and reboiler cannot be fixed and hence change with variations in throughput rates. To address this issue, the distillation columns were modified using a single-tower RadFrac model (without integrated condenser or reboiler) with a separate condenser and reboiler (heat exchangers, namely HeatX) as well as two splitters to recirculate the streams to the columns. This new combination is called the "decomposed model" in this work. The areas "A" of the condensers and reboilers of SR1, SR2 and TD could thus be fixed in the HeatX model at their nominal capacities according to Eqs. (2) and (3) (Towler and Sinnott, 2021). Heat duty "Q" and log-mean temperature difference "$LMTD$" were obtained at the nominal conditions. The overall heat transfer coefficient "U" was estimated following heuristics, based on the temperatures and liquid properties (Branan, 1998). The details are summarised in Appendix A.

$$Q = U * A * LMTD \tag{2}$$

$$LMTD = \frac{(Temp_{in} - temp_{out}) - (Temp_{out} - temp_{in})}{\ln\frac{Temp_{in} - temp_{out}}{Temp_{out} - temp_{in}}} \tag{3}$$

Where,

Q, heat duty, kJ/s
U, overall heat transfer coefficient, kJ/(s m^2 K)
$LMTD$, log-mean temperature difference, K
A, heat exchange surface area, m^2
$Temp_{in}$, inlet temperature of the hot stream, K
$Temp_{out}$, outlet temperature of the hot stream, K
$temp_{in}$, inlet temperature of the cold stream, K
$temp_{out}$, outlet temperature of the cold stream, K

After the decomposed models were constructed, the flowrates were varied. At different rates, split ratios between the reflux and distillate streams as well as between the boilup and bottom streams were adjusted to keep the purity and recovery yield of hexanoic acid in the outlet streams at the nominal conditions (deviation < 0.01 %). The utility usage was controlled by Design Specs. Here, it was assumed that for each equipment driven by electricity, its input flow rate was always proportional to its electricity consumption rate. Therefore, the minimum and maximum electricity consumption of the plant without any BESS (i.e., "$J_{\min}$" and "$J_{\max}$") could also be obtained, calculated as in Eqs. (4) and (5). They will be used in the evaluation of Cases 3–6.

$$J_{\min} = \max_i \frac{\dot{m}^i_{\min}}{\dot{m}^i_0} \times J_o \tag{4}$$

$$J_{\max} = \min_i \frac{\dot{m}^i_{\max}}{\dot{m}^i_0} \times J_o \tag{5}$$

where,

$J_{\min}$, minimum tolerable electricity supply of the plant, GJ/h
$J_{\max}$, maximum tolerable electricity supply of the plant, GJ/h
J_o, nominal electricity consumption of the plant, GJ/h

To assist volume flexibility at the equipment level, energy consumption (GJ/h) of the three columns were evaluated.

2.5.2. Plant level

2.5.2.1. Case 0. Since Case 0 was powered by constant grid electricity, it did not need a BESS to buffer the fluctuations in the electricity supply. Moreover, it essentially corresponds to the nominal conditions of the MES plant. Hence, volume flexibility is not applicable to Case 0.

2.5.2.2. Cases 1 and 2. In Cases 1 and 2, no BESS was deployed. As mentioned, for each equipment driven by electricity, its flow rate was assumed to be always linear to its electricity consumption rate. Therefore, in Cases 1 and 2, volume flexibility of the plant could be the frontier depicted by the most limiting *RECs* (see Eq. (6)).

$$LRR^k = REC^{SR1} \cap REC^{SR2} \cap REC^{TD} \tag{6}$$

where,

k, refer to Cases 1 or 2 here
LRR^k, load ratio range in Case k, %

2.5.2.3. Cases 3–6. In Cases 3–6, since a BESS was installed in the plant, the plant as a whole could consume extra electricity in addition to its nominal electricity consumption, or consume electricity when the production was off. Hence, the operating profile of the plant changed, and the "LRR^k" was quantified differently from using Eq. (6). Its boundaries were determined using Eq. (7), which were linked to the plant's

operating profile and thus the IRE profile. The operating profile consisted of the electricity stored into the BESS "Jin_t^k", the electricity discharged from the BESS "$Jout_t^k$", and the electricity directly used for production "J_t^k" (see the illustration in Fig. 3). For the IRE profile, we use "P_t^H" for explanation here, while the same rationale applies to "P_t^W" as well.

The lower boundary of "LRR^k" is defined as $\min V_{LB}^k$. It is the minimum "v/J_o" among the vector "V_{LB}^k". "v" is an available electricity power generated by the hybrid renewable electricity farm, which is time-independent. "J_o" is the hourly nominal electricity consumption of the MES plant. "V_{LB}^k" is composed of continuous "v/J_o" ratios (with a precision of 1%) that the "v" is equal to or smaller than the minimum electricity consumption of the MES plant without any BESS "$J_{\min}$" while the "C_v^k" equals to 100%. "C_v^k" represents the percentage of hours in a year the plant can fully consume the available electricity from the hybrid renewable electricity farm "$Jin_t^k + J_t^k = v = P_t^H$" as well as produce hexanoic acid "$J_t^k + Jout_t^k > J_{\min}$" over the hours when the "P_t^H" equals to a specific "v". To count the hours when this happens, the Iverson bracket "$[\![\Phi]\!]$" is used. If the statement Φ inside bracket is true, the value is 1, otherwise, 0. "$C_v^k = 100\%$" means that the plant can fully consume the available electricity from the hybrid renewable electricity farm and produce hexanoic acid whichever hour this electricity power "v" is generated by the hybrid renewable electricity farm "P_t^H" in a year.

The upper boundary of "LRR^k" is defined as "$\max V_{UB}^k$". It is the maximum "v/J_o" among the vector "V_{UB}^k". "V_{UB}^k" consists of a continuous range of "v/J_o" ratios (with a precision of 1%) that the "v" is equal to or larger than the maximum electricity consumption of the MES plant without any BESS "$J_{\max}$" while the "C_v^k" equals to 100%. Note that applying Eq. (7) to Cases 1 and 2 would get the same results as with Eq. (6).

$$LRR^k = [\min V_{LB}^k, \max V_{UB}^k]$$

s.t.

$$T = [1, 8760] \cap \mathbb{Z}$$

$$C_v^k = \frac{\sum_{t\in T} [\![Jin_t^k + J_t^k = v = P_t^H, J_t^k + Jout_t^k > J_{\min}]\!]}{\sum_{t\in T} [\![P_t^H = v]\!]} \quad , \forall v \in P_T^H$$

$$V_{LB}^k = \{\frac{v}{J_o} | v \leqslant J_{\min}, C^k_{\forall v^* \in [v, J_{\min}]} = 100\%\}$$

$$V_{UB}^k = \{\frac{v}{J_o} | v \geqslant J_{\max}, C^k_{\forall v^* \in [J_{\max}, v]} = 100\%\} \quad (7)$$

where,

T, vector of time, 1–8760 h

$\mathbb{Z}$, integers

v, available electricity power generated by the hybrid renewable electricity farm, time-independent, GJ/h

P_T^H, vector of available electricity from the hybrid renewable electricity farm over a year, GJ/h

C_v^k, the hours the plant can fully consume the available electricity and produce hexanoic acid over the hours this electrify power v generated by the hybrid renewable electricity farm over a year in case k, %

Jin_t^k, electricity stored to the BESS at time t in Case k, GJ/h

J_t^k, electricity directly used for production at time t in Case k, GJ/h

$Jout_t^k$, electricity discharged from the BESS at time t in Case k, GJ/h

P_t^H, available electricity from the hybrid renewable electricity farm at time t, GJ/h

V_{LB}^k, V_{UB}^k, vector of continuous v/J_o values (with a precision of 1 %) that satisfy the criteria for lower boundary and upper boundary, respectively, in case k, %

J_o, nominal electricity consumption of the MES plant without any BESS, GJ/h

v^*, available electricity power generated by the hybrid renewable electricity farm, time-independent (for intermediate calculation), GJ/h

To assist volume flexibility at the plant level, the shutdown time (h/y) and production quantity of hexanoic acid (kt/y) were also assessed. Shutdown time counts when "$J_t^k + Jout_t^k = 0$".

2.6. Economic assessment

Capital expenditure (CAPEX), operating expense (OPEX), and levelised production cost of hexanoic acid (LPC_{C6A}) were used to assess the economic performance of the plant's inside battery limits (i.e., process facility). The CAPEX was calculated as the sum of direct capital costs (i.e., purchase equipment cost), indirect capital costs (e.g., construction, supervision), and working capital costs. The purchase costs of equipment were either obtained from the Aspen Process Economic Analyzer v12, retrieved from vendors (e.g., ejectors), or estimated based on literature (e.g., MES). The direct costs and indirect costs were estimated using factors (e.g., a percentage of purchased equipment cost) available in references (Max et al., 2003; Sieder et al., 2004; Towler and Sinnott, 2021). A CAPEX flow might differ due to the replacement of BESS and LLE units at the end of year 15 as well as the salvage value of the whole plant at the end of its life, while the OPEX remains the same every year (assuming constant price of raw materials and utilities).

The OPEX includes costs for feedstock "F", electricity "E", utilities "UT", operation and maintenance "$O\&M$", and waste treatment "WT". Feedstock costs were calculated using the mass balance and feedstock's

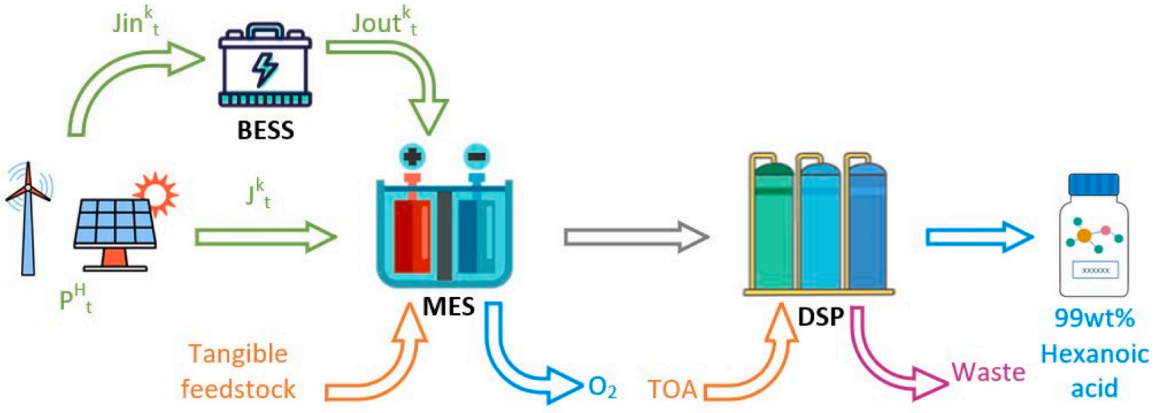

Fig. 3. Illustration of the operating profiles in Cases 3–6.

prices. Electricity and utility costs were calculated based on the energy balance of the plant and local energy prices. All the prices and assumptions to quantify CAPEX and OPEX can be found in Appendix A.

The LPC_{C6A} in all seven cases was calculated using Eq. (8). An economic allocation was applied between hexanoic acid and oxygen following Eq. (9). Thirty years of the plant's lifetime at a discount rate "*r*" of 8 % were assumed (Jourdin et al., 2020). The salvage value of the plant was assumed to be 3.3 % of the initial CAPEX (Jourdin et al., 2020; Kwan et al., 2018).

$$LPC^{k}_{C6A} = AF_{C6A}\frac{\sum_{y=1}^{n}\frac{CAPEX^{k}_{y}+O\&M^{k}+F^{k}+UT^{k}+WT^{k}+E^{k}}{(1+r)^{y}}}{\sum_{y=1}^{n}\frac{\dot{M}^{k}_{C6A}}{(1+r)^{y}}} \quad (8)$$

$$AF_{C6A} = \frac{\dot{M}^{0}_{C6A}\theta_{C6A}}{\dot{M}^{0}_{C6A}\theta_{C6A}+\dot{M}^{0}_{O_2}\theta_{O_2}} \quad (9)$$

where,

LPC^{k}_{C6A}, levelised production cost of hexanoic acid in Case *k*, €/kg

n, plant lifetime in years

y, year

$CAPEX^{k}_{y}$, capital expenditure in year *y* and in Case *k*, M€/y

O&M^{k}, annual operation and maintenance costs in Case *k*, M€/y

F^{k}, feedstock cost in Case *k*, M€/y

UT^{k}, utilities cost in Case *k*, M€/y

WT^{k}, waste treatment cost in Case *k*, M€/y

E^{k}, electricity cost in Case *k*, M€/y

r, discount rate. %

$\dot{M}^{k}_{C6A}$, mass flow rate of hexanoic acid in a year in Case k, kt/y

$\dot{M}^{0}_{O_2}, \dot{M}^{0}_{C6A}$, mass flow rate of oxygen and hexanoic acid in Case 0, respectively, kt/y

AF_{C6A}, economic allocation factor of hexanoic acid

$\theta_{O_2}, \theta_{C6A}$, market price of oxygen and hexanoic acid, respectively, €/kg

3. Results and discussion

3.1. Process modelling at the nominal conditions

Table 3 summarises the techno-economic results of the MES plant without a BESS at the nominal conditions, i.e., results of Case 0. The production of hexanoic acid required much more electric energy than energy from the hot utilities. This is not surprising given the electricity consumption of the electrolyser, which is at the core of the concept. Among the hot utilities, low-pressure steam yielded a negative value, indicating that there was more generation of this utility than consumption. The net amount of this utility was partially used for the low-low-pressure steam demand and partially used outside the plant without profit. The annual consumption of CO_2 was 23 kt/y. Therefore, the electricity required to convert a tonne of CO_2 into hexanoic acid was 24.7 GJ/t (= 6.9 MWh/t). Detailed utilities and electricity consumption and a complete stream table can be found in Appendix B.

Table 3
Techno-economic results in Case 0 (prices in 2019).

Technical indicators	Value
Utilities	
Low-low-pressure steam – TJ/y	3.7
Low-pressure steam – TJ/y	-20.1
Hot oil – TJ/y	217.4
Medium-pressure steam – TJ/y	11.2
Chilled water – TJ/y	61.7
Cooling water – TJ/y (kt/y)	144 (2302)
Electricity consumption – TJ/y (=GWh/y)	**600 (=167)**
Economic indicators	**Value**
CAPEX – M€	**93**
Fixed capital investment – M€	79
Working capital – M€	14
OPEX – M€/y	**34**
Operations and maintenance – M€/y	9.5
Feedstock – M€/y	6.7
Electricity – M€/y	15.4
Utilities (incl. cooling water) – M€/y	0.9
Waste treatment – M€/y	1.6
Levelised production cost of hexanoic acid, LPC^{0}_{C6A} – €/kg	**4.0**

Among all the items contributing to the OPEX, the annual electricity cost was the highest, accounting for 36 %, followed by operations and maintenance costs (22 %) and feedstock (20 %). The levelised production cost of hexanoic acid, LPC^{0}_{C6A} was estimated at 4.0 €/kg, which was 33 % higher than the assumed market price (i.e., 3 €/kg for 2019), but still fell within the range of current market prices of hexanoic acid (i.e., 2.5–4.2 €/kg) (Dessi et al., 2021).

3.2. Volume flexibility

3.2.1. Equipment level

Table 4 summarises the *REC* of the three process columns and pinpoints the bottlenecks for the reference. The bottlenecks were the pieces of equipment that limit the minimum and maximum values of throughput rate for each distillation column; these were the condenser and the tower (tray's hydraulic performance was affected).

The dimensions of condensers were fixed at the nominal conditions. During the test to estimate volume flexibility at a lower throughput rate, the reflux and boilup ratios were adjusted to maintain the same temperature profile inside the tower as under nominal conditions (to obtain the targeted product streams). The resulting throughput rate of the condenser declined, and the value of *Q* decreased. Since the *U*, *A*, and the conditions of utilities were fixed (e.g., inlet and outlet temperature, steam ratio), *LMTD* was forced to be reduced gradually. It would eventually reach the minimum temperature difference and thus the minimum heat duty limited by the initial design. Moreover, according to Eq. (3), the decrease of *LMTD* marks a reduction in $Temp_{out}$ of the condenser, which might affect the operating conditions of the next unit. Therefore, to allow a lower throughput rate, an extra heater should be installed to amend the deviation of $Temp_{out}$ in avoidance of possible failure of subsequent unit operations. At a larger throughput rate, the distillate stream cannot be fully condensed. In a future design, overdesigning the condensers is an option to perform for larger ranges of throughput rates. More explicitly, the overdesign factor allowed for a heat exchanger in the industry is normally within 20 % to avoid fouling (Bennett et al., 1973; Shah and Sekuli, 2003). Another option is to increase the initial temperature difference between the target cooling or heating stream and the utility used.

The performance of the tray's hydraulics also appeared as a bottleneck. It was reported as low loading rate in Aspen. The loading rate in the tower is calculated as the rate of liquid that is split from the condensed overhead stream and that is sent back to the tower, which is associated with the reflux ratio. The internal geometry of the tower

Table 4
Summary of volume flexibility limits at equipment level and its bottlenecks. REC: range of effective capacity. SR: solvent regeneration. TD: dehydration column.

Equipment	REC	Lower boundary bottleneck	Higher boundary bottleneck
SR1	[56%, 100%]	Condenser oversized	Condenser undersized
SR2	[65%, 100%]	Tray's hydraulic performance	Condenser undersized
TD	[70%, 100%]	Tray's hydraulic performance	Condenser undersized

imposes to a minimum threshold loading rate for the trays. When the inlet flow rate keeps declining, it eventually results in a low loading rate. The liquid was held up on the upper stages by the gas, leading to undesired operating conditions.

Operating the distillation columns at lower throughput rates than the nominal rate results in an increase in energy consumption per tonne hexanoic acid produced. The highest increase occurs in the final dehydration column TD. At the point when its throughput rate reaches the lowest possible value of 70 % of its nominal rate, its energy consumption per tonne hexanoic acid produced increased maximally: 8 % compared to its nominal conditions. This finding coheres to the reality in industry, which usually reports higher variations. However, in this work, compared to the total energy consumption, the variation can be considered negligible. Refer to Appendix A for further details.

3.2.2. Plant level

3.2.2.1. Cases 1 and 2. The volume flexibility results of Cases 1 and 2 are presented in Table 5. No BESS was implemented in these two cases, so the plant had to be shut down for 44 % and 31 % of the nominal operating time per year (i.e., 8760 h/y), respectively. The resulting production quantity of hexanoic acid was 47 % and 34 % lower than the nominal production target. Case 2 performed better because it was coupled with the hybrid electricity profile, which supplies more electricity throughout the year. In terms of volume flexibility, in both cases, the plant could fully consume available electricity and operate safely while satisfying the product purity and recovery yield when the available electricity was 70 % and 100 % of the plant's nominal electricity consumption. Below 70 %, the plant always had to be shut down.

3.2.2.2. Cases 3–6. A BESS was installed in the MES plant in Cases 3–6. To reflect the impact of operating schemes, Cases 3 and 5 or 4 and 6 are compared in Fig. 4. As the deployed capacity of BESS increased, the shutdown time was reduced and the production quantity increased more rapidly under operating scheme 1. Moreover, under scheme 1, the results indicate that to completely avoid shutting down the plant by covering all the long periods of electricity shortage, a minimum BESS capacity of 12.5 TJ/h (=3.5 GW) would be required in Case 3 and of 1.7 TJ/h (=0.47 GW) in Case 4 (note these numbers are not plotted in the figure). The corresponding values would be higher under scheme 2.

As for the impact of a BESS on volume flexibility, the lower boundary of LRR^k could only be slightly expanded as the BESS capacity increased under scheme 1. Therefore, the improvement in volume flexibility was insignificant. This result implies that in this context, selected BESS capacities and operating schemes could not expand the range of available electricity that can be fully consumed by the plant while safely producing hexanoic acid that satisfied the product purity and recovery requirements. On the other hand, to provide more details regarding how shortage hours were partially covered with the help of a BESS, an example is provided to demonstrate the conditions of coverage percentage of shortage hours "C_v^k" versus electricity power generated by the renewable electricity farm over nominal electricity consumption of the reference process "v/J_o". For instance, in Case 4 (see Fig. 5), at a BESS capacity of 20 GJ/h (=5.6 MW), the MES plant could partially cover shortage hours "$100\% > C_v^4 > 0$" when the available electricity power was between 40% and 69% of its nominal electricity consumption rate "$69\% \geq v/J_o \geq 40\%$". This partial coverage accounted for the decrease in shutdown time and the increase in production quantity.

Another common trend between shutdown time and production quantity under scheme 1, was that the decreasing or increasing trend plateaued locally as the BESS capacity approached 50 GJ/h. This indicates the existence of a hurdle for deploying BESS at a certain point. This is essentially related to the long periods of electricity shortage. A BESS installation of 50 GJ/h was only enough to cover short periods of electricity shortage. Moreover, under operating scheme 1, little extra electricity was taken in by the plant equipped with a BESS. This is confirmed by the right part of Fig. 5. When the "v/J_o" was above 100%, meaning when there was extra electricity, the "C_v^4" was small. Regarding operating scheme 2, it performed worse in any of the three indicators.

To summarise, an operating scheme where the BESS could be charged at peak hours and used to cover electricity shortage periods was more effective in improving overall production quantity, when compared to an operating scheme where the BESS can only be charged at off-peak hours and used for increasing the production as soon as possible. However, even under the first operating scheme, the benefits from a BESS will eventually plateau locally when its capacity increases, due to the long periods of electricity shortage.

As for the impact of different electricity profiles on technical performances, Cases 3 and 4 or Cases 5 and 6 can be compared. Undoubtedly, the cases where hybrid electricity was supplied performed better, as the hybrid electricity profile consists of solar and wind electricity, which renders a higher average capacity. Otherwise, the trends were the same for all technical indicators.

Table 5
Results of Cases 1 and 2.

	Case 1	Case 2
Shutdown time (h/y)	3837	2678
Production quantity (kt/y)	5.4	6.7
LRR^k	[70 %, 100 %]	[70 %, 100 %]

3.3. Economic performance

The economic results of Cases 1–6 are shown in Fig. 6. Comparing Cases 1 and 2 to Case 0, the levelised production cost of hexanoic acid (LPC_{C6A}^k) was penalised by 34% and 19%, respectively, owing to the reduced production quantity and therefore less revenue. In both cases, the shares related to capital goods (i.e., O&M and CAPEX) increased while the shares relevant to daily operation decreased (i.e., the rest).

To compare the impact caused by different operating schemes, Cases 3 and 5 or Cases 4 and 6 should be compared to each other. Under operating scheme 1 (i.e., Cases 3 and 4), initially, the BESS contributed to decrease the LPC_{C6A}. In Case 3, the LPC_{C6A}^3 went down to 5.1 €/kg when the capacity of BESS was 29 GJ/h (=8.1 MW), leading to an improvement of 4% compared to Case 1. In Case 4, the lowest LPC_{C6A}^4 reached was 4.7 €/kg with a BESS of 12 GJ/h (=3.3 MW), which was improved by less than 1% upon Case 2. Compared to LPC_{C6A}^0, the penalty in production cost was 28% in Case 3 and 18% in Case 4. Meanwhile, the shares of CAPEX and O&M costs first declined and then increased along with the increase in the BESS capacity. This trend points out that a higher BESS capacity does not guarantee a lower LPC_{C6A}. This was due to the fact that the extra production of hexanoic acid was not always linear to the BESS capacity, as visualised in Fig. 4. Therefore, at a certain point, the increased capital investment in BESS could not be paid back by the limited extra revenue. Under operating scheme 2 (see Cases 5 and 6), the LPC_{C6A}^5 and LPC_{C6A}^6 as well as the shares of CAPEX and O&M costs raised proportionally to the BESS capacity, which suggests that the installation of BESS did not enhance the economic viability under this scheme. The reason was that the use of the BESS was restricted, which is capital intensive and thereby resulting in a high sunk cost. This finding is in line with other similar studies (Prevoteau et al., 2020; Wood et al., 2021). Moreover, similar to the technical performances, different electricity profiles did have an impact on the values but not on the trends.

4. Conclusions

The current paper conducts an ex-ante assessment of a novel MES process for synthesising hexanoic acid under IRE supply. This paper aims to (i) contribute to volume flexibility estimation, (ii) elucidate the

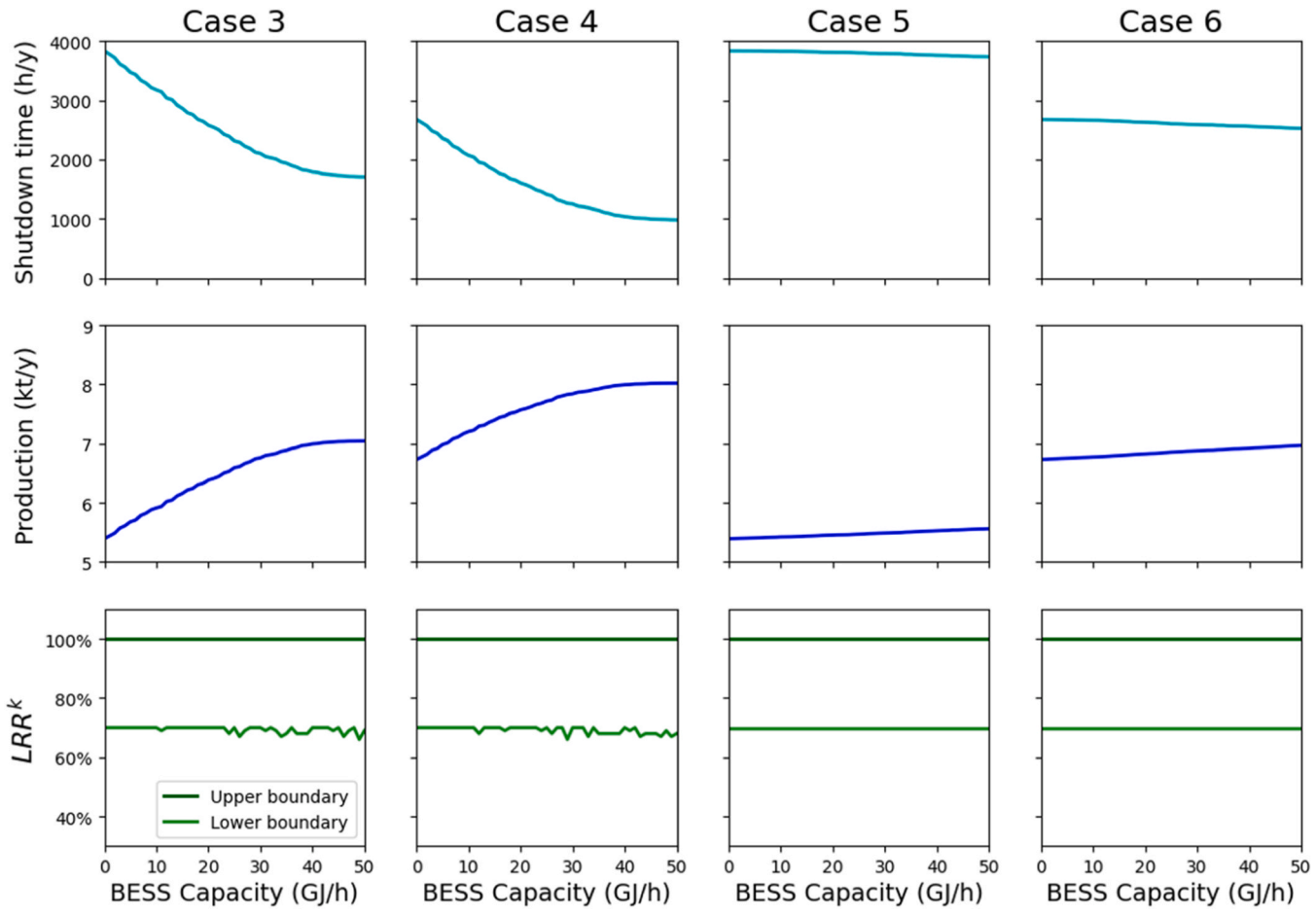

Fig. 4. Shutdown time, production quantity of hexanoic acid, and loa ratio range (LRR) in Cases 3–6.

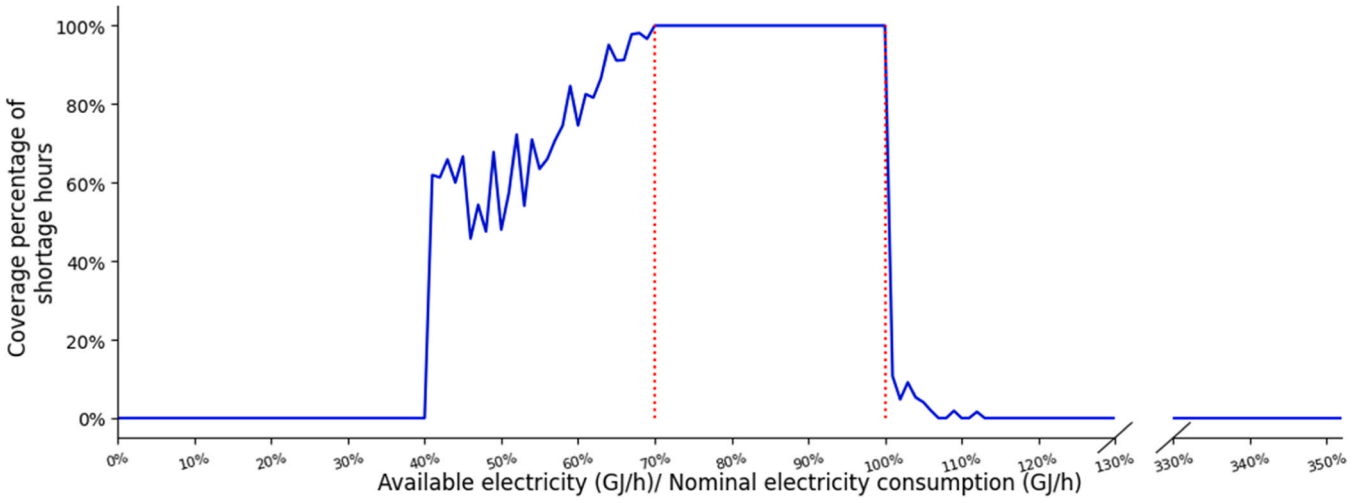

Fig. 5. Coverage percentage of shortage hours "C_v^4" versus available electricity over nominal electricity consumption of the reference process "v/J_o". An example of Case 4 with a BESS of 20 GJ/h. Red dashed lines: boundaries of LRR^4 with a BESS of 20 GJ/h.

impact of intermittency on the techno-economic performance of a MES plant, (iii) and understand the use of batteries as a strategy to improve the performance of the plant.

At the equipment level, the sizing of condensers and the internal geometrical design of the tower were identified as bottlenecks in the volume flexibility of the separation columns. To enhance the volume flexibility of condensers, three options are recommended: 1) deploy condensers and reboilers that allow a smaller minimum heat duty; 2) overdesign, or 3) increase the initial temperature difference between the target cooling or heating stream and utility stream. Moreover, operating the equipment below its nominal rates penalises the utility consumption. Regarding the internal design of the tower and trays, a better design of column's internal geometry or a higher reflux ratio could enhance their volume flexibility. Eventually, based on the results at the equipment

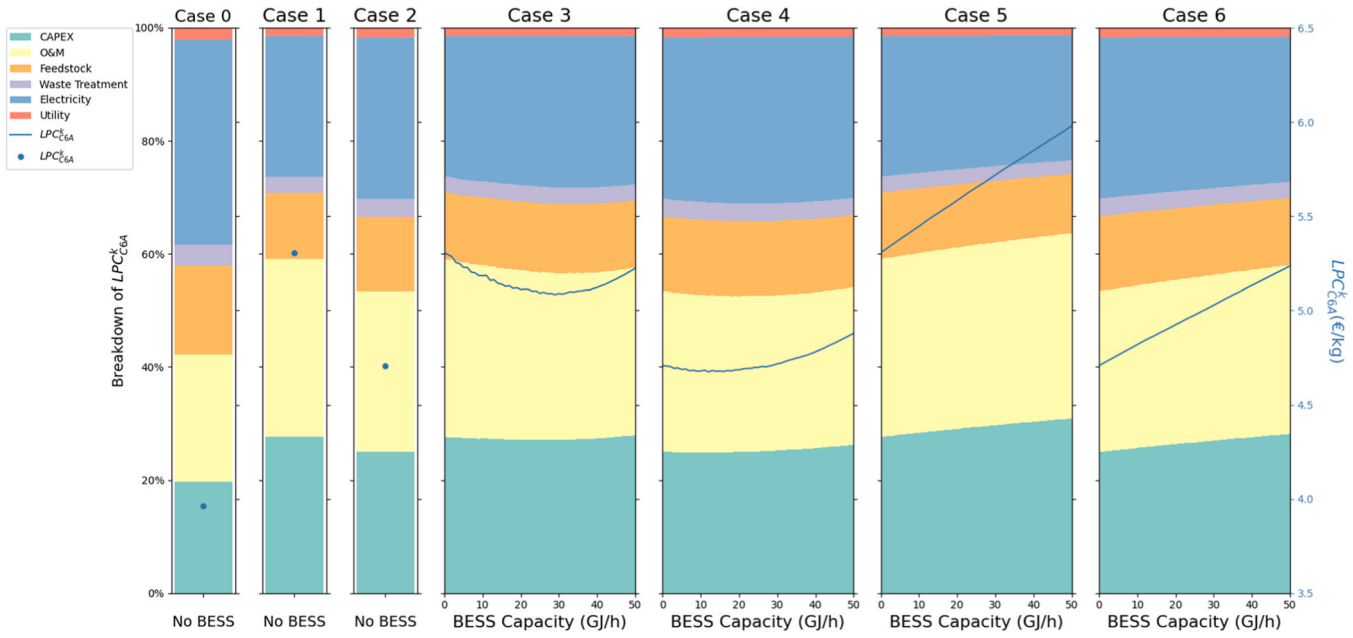

Fig. 6. Levelised production cost of hexanoic acid and its breakdown versus a range of BESS capacities.

level, in this work, column TD restricted the volume flexibility of the entire plant.

At the plant level and nominal conditions (i.e., Case 0), the levelised production cost of hexanoic acid (LPC^{0}_{C6A}) was 4.0 €/kg, which is competitive in today's market. When the electricity source was switched from constant grid electricity to IRE without implementing flexibility strategies (i.e., Cases 1 and 2), the LPC_{C6A} was penalised by 34% and 19%, respectively. It was a consequence of shutting down the plant for 44% and 31% of the time per year due to electricity shortage. Batteries could help to reduce the penalties in production quantity. However, under an operating scheme where the batteries can be charged during peak hours and primarily used to cover the shortage (i.e., Cases 3 and 4), the penalties in LPC_{C6A} was not exaggerated only when short periods of electricity shortage were covered. Otherwise, the capital investment in batteries became too large to be compensated by the revenue obtained from the increase in hexanoic acid production. Moreover, under the operating scheme where the batteries can only be charged during off-peak hours (i.e., Cases 5 and 6), the batteries were not used enough owing to the stringent operating scheme. Consequently, the batteries barely increased the production time, and the limited additional revenue could not pay back the capital investment. In any case, coupling the MES plant with IRE is not economically viable in this context.

For future work, along with the development of the MES technology, more details of the technologies should be included, such as more realistic assumptions and estimations. Also, it should be highlighted that the solvent regeneration and distillation unit operations should be validated by experiments or pilots in the future. Moreover, novel extraction technologies for dilute VCAs, such as electrodialysis, can be considered and incorporated into the simulation model when they become more mature. Other design strategies to improve volume flexibility can also be studied. In addition, operating schemes, namely the scheduling of the plant, can be optimised while maximising the production. Importantly, the environmental performance should also be assessed to understand the impact and potential of the technology.

Declaration of Competing Interest

The authors declare that they have no known competing financial interests or personal relationships that could have appeared to influence the work reported in this paper.

Acknowledgements

This work was supported by Shell and a PPP-allowance from Top Consortia for Knowledge and Innovation (TKI's) of the Dutch Ministry of Economic Affairs and Climate Policy in the context of the TU Delft e-Refinery Institute. MPF acknowledges the financial support of the NWO ECCM tenure track grant "Addressing the multiscale challenge of CO_2 electrochemical reduction" (project number ECCM.TT.009) which is (partly) financed by the Dutch Research Council (NWO).

Appendix A. Supporting information

Supplementary data associated with this article can be found in the online version at doi:10.1016/j.cherd.2024.04.005.

References

Aghapour Aktij, S., Zirehpour, A., Mollahosseini, A., Taherzadeh, M.J., Tiraferri, A., Rahimpour, A., 2020. Feasibility of membrane processes for the recovery and purification of bio-based volatile fatty acids: a comprehensive review. J. Ind. Eng. Chem. 81, 24–40. https://doi.org/10.1016/j.jiec.2019.09.009.

Ajah, A.N., Herder, P.M., 2005. Addressing flexibility during process and infrastructure systems conceptual design: real options perspective. IEEE Sys. Man Cybern. 3711–3716. https://doi.org/10.1109/ICSMC.2005.1571723.

Atasoy, M., Owusu-Agyeman, I., Plaza, E., Cetecioglu, Z., 2018. Bio-based volatile fatty acid production and recovery from waste streams: current status and future challenges. Bioresour. Technol. 268, 773–786. https://doi.org/10.1016/j.biortech.2018.07.042.

Benalcázar, E.A., Deynoot, B.G., Noorman, H., Osseweijer, P., Posada, J.A., 2017. Production of bulk chemicals from lignocellulosic biomass via thermochemical conversion and syngas fermentation: a comparative techno-economic and environmental assessment of different site-specific supply chain configurations. Biofuels, Bioprod. Bioref. 11, 861–886. https://doi.org/10.1002/bbb.1790.

Bennett, C.A., Kistler, R.S., Lestina, T.G., 1973. Influence of stochastic inputs and parameters on heat-exchanger design. Ind. Eng. Chem. Proc. Dd. 12, 165–170. https://doi.org/10.1021/i260046a007.

Branan, C.R., editor. Rules of thumb for chemical engineers. 3rd ed. USA: Gulf Publishing Company; 1998.

Brée, L.C., Bulan, A., Herding, R., Kuhlmann, J., Mitsos, A., Perrey, K., Roh, K., 2020. Techno-Economic Comparison of Flexibility Options in Chlorine Production. Ind. Eng. Chem. Res. 59, 12186–12196. https://doi.org/10.1021/acs.iecr.0c01775.

Canapi, E.C., Agustin, Y.T.V., Moro, E.A., Pedrosa, E., Bendaño, Ma.L.J., 2005. Coconut Oil. In: Shahidi, F. (Ed.), Bailey's Industrial Oil and Fat Products, 6th ed. John Wiley & Sons, USA, pp. 123–147.

Cavalcante, W.D., Leitao, R.C., Gehring, T.A., Angenent, L.T., Santaella, S.T., 2017. Anaerobic fermentation for n-caproic acid production: A review. Process Biochem 54, 106–119. https://doi.org/10.1016/j.procbio.2016.12.024.

Chen, C., Yang, A.D., 2021. Power-to-methanol: The role of process flexibility in the integration of variable renewable energy into chemical production. Energy Convers. Manag. 228. https://doi.org/10.1016/j.enconman.2020.113673.
Chen, Z., Wang, X., Liu, L., 2019. Electrochemical reduction of carbon dioxide to value-added products: the electrocatalyst and microbial electrosynthesis. Chem. Rec. 19, 1272–1282. https://doi.org/10.1002/tcr.201800100.
Christodoulou, X., Okoroafor, T., Parry, S., Velasquez-Orta, S.B., 2017. The use of carbon dioxide in microbial electrosynthesis: advancements, sustainability and economic feasibility. J. CO2 Util. 18, 390–399. https://doi.org/10.1016/j.jcou.2017.01.027.
Christodoulou, X., Velasquez-Orta, S.B., 2016. Microbial electrosynthesis and anaerobic fermentation: an economic evaluation for acetic acid production from CO2 and CO. Environ. Sci. Technol. 50, 11234–11242. https://doi.org/10.1021/acs.est.6b02101.
De Luna, P., Hahn, C., Higgins, D., Jaffer, S.A., Jaramillo, T.F., Sargent, E.H., 2019. What would it take for renewably powered electrosynthesis to displace petrochemical processes. Science 364. https://doi.org/10.1126/science.aav3506.
Del Pilar Anzola Rojas, M., Zaiat, M., Gonzalez, E.R., De Wever, H., Pant, D., 2018. Effect of the electric supply interruption on a microbial electrosynthesis system converting inorganic carbon into acetate. Bioresour. Technol. 266, 203–210. https://doi.org/10.1016/j.biortech.2018.06.074.
Dessi, P., Rovira-Alsina, L., Sanchez, C., Dinesh, G.K., Tong, W., Chatterjee, P., Tedesco, M., Farras, P., Hamelers, H.M.V., Puig, S., 2021. Microbial electrosynthesis: Towards sustainable biorefineries for production of green chemicals from CO2 emissions. Biotechnol. Adv. 46, 107675 https://doi.org/10.1016/j.biotechadv.2020.107675.
Eneco [Internet]. Windpark Slufterdam. https://www.eneco.nl/over-ons/wat-we-doen/duurzame-bronnen/windpark-slufterdam/; 2022 [accessed 11 Nov 2022].
Commission Delegated Regulation (EU) 2023/1184 of 10 February 2023. (2023).
Gadkari, S., Mirza Beigi, B.H., Aryal, N., Sadhukhan, J., 2021. Microbial electrosynthesis: is it sustainable for bioproduction of acetic acid? RSC Adv. 11, 9921–9932. https://doi.org/10.1039/d1ra00920f.
Gadkari, S., Shemfe, M., Modestra, J.A., Mohan, S.V., Sadhukhan, J., 2019. Understanding the interdependence of operating parameters in microbial electrosynthesis: a numerical investigation. Phys. Chem. Chem. Phys. 21, 10761–10772. https://doi.org/10.1039/c9cp01288e.
Grossmann, I.E., Sargent, R.W.H., 1978. Optimum design of chemical-plants with uncertain parameters. Aiche J. 24, 1021–1028 https://doi.org/DOI.10.1002/aic.690240612.
Huesman, A., 2020. Integration of operation and design of solar fuel plants: A carbon dioxide to methanol case study. Comput. Chem. Eng. 140, 106836 https://doi.org/10.1016/j.compchemeng.2020.106836.
Huq, N.A., Hafenstine, G.R., Huo, X., Nguyen, H., Tifft, S.M., Conklin, D.R., Stuck, D., Stunkel, J., Yang, Z., Heyne, J.S., Wiatrowski, M.R., Zhang, Y., Tao, L., Zhu, J., McEnally, C.S., Christensen, E.D., Hays, C., Van Allsburg, K.M., Unocic, K.A., Meyer, H.M., Abdullah 3rd, Z., Vardon, D.R., 2021. Toward net-zero sustainable aviation fuel with wet waste-derived volatile fatty acids. PNAS 118. https://doi.org/10.1073/pnas.2023008118.
IPCC. Climate change 2022: Impacts, adaptation and vulnerability. 2022. https://doi.org/10.1017/9781009325844.
Jones, R.J., Massanet-Nicolau, J., Guwy, A.J., 2021. A review of carboxylate production and recovery from organic wastes. Bioresour. Technol. Rep. 16, 100826 https://doi.org/10.1016/j.biteb.2021.100826.
Jourdin, L., Sousa, J., van Stralen, N., Strik, D.P.B.T.B., 2020. Techno-economic assessment of microbial electrosynthesis from CO2 and/or organics: An interdisciplinary roadmap towards future research and application. Appl. Energy 279, 115775. https://doi.org/10.1016/j.apenergy.2020.115775.
Kwan, T.H., Hu, Y.Z., Lin, C.S.K., 2018. Techno-economic analysis of a food waste valorisation process for lactic acid, lactide and poly(lactic acid) production. J. Clean. Prod. 181, 72–87. https://doi.org/10.1016/j.jclepro.2018.01.179.
Luo, J., Moncada, J., Ramirez, A., 2022. Development of a conceptual framework for evaluating the flexibility of future chemical processes. Ind. Eng. Chem. Res. 61, 3219–3232. https://doi.org/10.1021/acs.iecr.1c03874.
Max, S.P., Klaus, D.T., Ronald, E.W., 2003. Plant design and economics for chemical engineers, 5th ed. McGraw-Hill Companies, Boston.
McNamara, M., Plutshack, V., Phillips, J., Poindexter, N. [Internet]. Can Time-of-Use Tariffs Increase the Financial Viability of Mini-Grids? https://dukespace.lib.duke.edu/dspace/bitstream/handle/10161/26572/can-time-of-use-tariffs-increase-financial-viability.pdf?sequence=2; 2022 [accessed 11 Nov 2022].
Miller, J.H., Hafenstine, G.R., Nguyen, H.H., Vardon, D.R., 2022. Kinetics and Reactor Design Principles of Volatile Fatty Acid Ketonization for Sustainable Aviation Fuel Production. Ind. Eng. Chem. Res. 61, 2997–3010. https://doi.org/10.1021/acs.iecr.1c04548.
Morgenthaler, S., Kuckshinrichs, W., Witthaut, D., 2020. Optimal system layout and locations for fully renewable high temperature co-electrolysis. Appl. Energy 260, 114218. https://doi.org/10.1016/j.apenergy.2019.114218.
Osman, O., Sgouridis, S., Sleptchenko, A., 2020. Scaling the production of renewable ammonia: A techno-economic optimization applied in regions with high insolation. J. Clean. Prod. 271, 121627 https://doi.org/10.1016/j.jclepro.2020.121627.
Prevoteau, A., Carvajal-Arroyo, J.M., Ganigue, R., Rabaey, K., 2020. Microbial electrosynthesis from CO2: forever a promise. Curr. Opin. Biotechnol. 62, 48–57. https://doi.org/10.1016/j.copbio.2019.08.014.
Qi, M., Park, J., Landon, R.S., Kim, J., Liu, Y., Moon, I., 2022. Continuous and flexible Renewable-Power-to-Methane via liquid CO2 energy storage: Revisiting the techno-economic potential. Renew. Sustain. Energy Rev. 153. https://doi.org/10.1016/j.rser.2021.111732.
Saboe, P.O., Manker, L.P., Michener, W.E., Peterson, D.J., Brandner, D.G., Deutch, S.P., Kumar, M., Cywar, R.M., Beckham, G.T., Karp, E.M., 2018. In situ recovery of bio-based carboxylic acids. Green. Chem. 20, 1791–1804. https://doi.org/10.1039/c7gc03747c.
Sadhukhan, J., Lloyd, J.R., Scott, K., Premier, G.C., Yu, E.H., Curtis, T., Head, I.M., 2016. A critical review of integration analysis of microbial electrosynthesis (MES) systems with waste biorefineries for the production of biofuel and chemical from reuse of CO 2. Renew. Sustain. Energy Rev. 56, 116–132. https://doi.org/10.1016/j.rser.2015.11.015.
Shah, R.K., Sekuli, D.P., 2003. Fundamentals of Heat Exchanger Design, 1st ed. John Wiley & Sons, USA.
Shell [Internet]. Shell opens solar park at Shell Moerdijk chemicals site in the Netherlands. https://www.shell.com/business-customers/chemicals/media-releases/2019-media-releases/shell-moerdijk-solar-farm.html; 2019 [accessed 11 Nov 2022].
Shemfe, M., Gadkari, S., Yu, E., Rasul, S., Scott, K., Head, I.M., Gu, S., Sadhukhan, J., 2018. Life cycle, techno-economic and dynamic simulation assessment of bioelectrochemical systems: A case of formic acid synthesis. Bioresour. Technol. 255, 39–49. https://doi.org/10.1016/j.biortech.2018.01.071.
Sieder, W., Seader, J., Lewin, D., 2004. Product and process design principles, 3rd ed. John Wiley & Sons, USA.
Staffell, I., Pfenninger, S., 2016. Using bias-corrected reanalysis to simulate current and future wind power output. Energy 114, 1224–1239. https://doi.org/10.1016/j.energy.2016.08.068.
Statista [Internet]. Prices of electricity for non-household consumers in the Netherlands. https://www.statista.com/statistics/596254/electricity-industry-price-netherlands/#:~:text=The%2010.51%20euro%20cents%20per,towards%20the%20middle%2Drange%20of; 2022 [accessed 11 Nov 2022].
The Dollar Business Bureau [Internet]. India lifts 9-year ban on bulk export of certain edible oils. https://www.thedollarbusiness.com/news/india-removes-ban-on-bulk-export-of-certain-edible-oils/49790; 2017 [accessed 10 Aug 2022].
Towler, G., Sinnott, R., 2021. Chemical engineering design: principles, practice and economics of plant and process design, 2nd ed. Butterworth-Heinemann, Amsterdam.
Valentino, L., Alejandre, A., 2023. Capacitive Deionization for the Extraction and Recovery of Butyrate. Acs Sustain Chem. Eng. 11, 6385–6394. https://doi.org/10.1021/acssuschemeng.3c00221.
Wang, G.H., Mitsos, A., Marquardt, W., 2020. Renewable production of ammonia and nitric acid. Aiche J. 66, e16947 https://doi.org/10.1002/aic.16947.
Whitehead, R. [Internet]. El Niño disruption causes palm kernel prices to double. https://www.foodnavigator-asia.com/Article/2017/01/16/El-Nino-disruption-causes-palm-kernel-prices-to-double; 2017 [accessed.
Woo, H.C., Kim, Y.H., 2019. Eco-efficient recovery of bio-based volatile C2-6 fatty acids. Biotechnol. Biofuels 12, 92. https://doi.org/10.1186/s13068-019-1433-8.
Wood, J.C., Grove, J., Marcellin, E., Heffernan, J.K., Hu, S., Yuan, Z., Virdis, B., 2021. Strategies to improve viability of a circular carbon bioeconomy-A techno-economic review of microbial electrosynthesis and gas fermentation. Water Res 201, 117306. https://doi.org/10.1016/j.watres.2021.117306.
Zhang, T., Tremblay, P.-L., 2019. Possible industrial applications for microbial electrosynthesis from carbon dioxide, microbial electrochemical. Technology 825–842.